Environmental Pollution 252 (2019) 1170–1179

Contents lists available at ScienceDirect

Environmental Pollution

journal homepage: www.elsevier.com/locate/envpol

The influence of roadside trees on the diffusion of road traffic pollutants and their magnetic characteristics in a typical semi-arid urban area of Northwest China

Hong Chen [a], Bo Wang [b,*], Dun-sheng Xia [a], Yi-jiao Fan [a], Hui Liu [a], Zhi-rong Tang [a], Shan Ma [a]

[a] Key Laboratory of Western China's Environmental Systems (Ministry of Education), College of Earth and Environmental Sciences, Lanzhou University, Lanzhou, 730000, China

[b] College of Geography and Environmental Sciences, Zhejiang Normal University, Jinhua, 321004, China

ARTICLE INFO

Article history:
Received 29 December 2018
Received in revised form
6 June 2019
Accepted 6 June 2019
Available online 7 June 2019

Keywords:
Biomagnetic monitoring
Road pollution
Elemental concentrations
Tree configuration

ABSTRACT

Leaf samples of *Juniperus formosana* were collected from an open road environment, in order to establish how particulate matter (PM) generated by vehicles was dispersed in both horizontal and vertical directions. Sampling was conducted at sites with trees of varying height and configuration adjacent to a major road in Lanzhou, Gansu Province, Northwest China. The concentration of remanence-bearing ferrimagnets in the leaf samples was estimated from measurements of Saturation Isothermal Remanent Magnetization (SIRM), while the weight of particles deposited on the leaves and their elemental composition were determined at different heights and in different directions relative to the road. The PM on the surface of needles was predominantly influenced by traffic emissions and by dust resuspension. Rows of roadside trees, as opposed to solitary trees, were more effective at intercepting PM and thus in filtering road traffic pollution. The results indicate that *Juniperus formosana* needles may be an effective bio-sensor for monitoring variations in the spatial diffusion of road pollutants.

1. Introduction

Long-term exposure to high levels of urban atmospheric particulate matter (PM), especially that related to road traffic pollutants, may have serious health effects such as damage to the central nervous (Huang and Guo, 2014), cardiovascular (Hart et al., 2013; Wu et al., 2013; Wu et al., 2012), respiratory (Jones et al., 2006) and reproductive systems (Huang and Guo, 2014). In addition, air pollutants deposited on the surface of leaves are rich in potentially toxic heavy metals such as lead and zinc which may have adverse ecological effects (Ram et al., 2015), such as the inhibition of photosynthesis, leaf senescence (Burkhardt, 2010), increased stomatal density (Kardel et al., 2010; Simon et al., 2014), pigment degradation (Prusty et al., 2005), and the degradation of epicuticular waxes. Specifically, these effects may lead to decreased drought tolerance (Burkhardt and Pariyar, 2014). Moreover, fine PM, with an enhanced heavy metal content, trapped on leaf surfaces will be continuously accumulated. Under severe air disturbance or interference by human factors, the accumulated dust on leaf surfaces will enter the atmosphere and produce secondary pollution. Consequently, the monitoring of the sources and diffusion characteristics of pollutants from the road environment needs to be urgently undertaken, and solutions need to be found in order to curtail the propagation of PM emitted from road traffic in urban areas (Karagulian et al., 2015). Previous results showed that urban greening results in the capture of atmospheric PM, and that it can be carried out on a micro-scale due to plant leaves typically having a large surface area which can intercept PM (Litschke and Kuttler, 2008). Leaves act as a natural accumulator of PM and analysis of their biomagnetic properties can reveal the severity of traffic pollution at a high spatial resolution (Gautam et al., 2005; Hofman et al., 2013; Hofman et al., 2014a; Hofman et al., 2014b; Moreno et al., 2003; Prajapati et al., 2006; Rai, 2013; Szönyi et al., 2007; Urbat et al., 2004). An advantage of this type of biomagnetic monitoring is that the host leaves are non-magnetic and thus the concentration of remanence-bearing ferrimagnets estimated by

This paper has been recommended for acceptance by Admir Créso Targino

* Corresponding author. 688#, Yingbin Road, Zhejiang Normal University, Jinhua, Zhejiang Province, 321004, PR China.

E-mail address: bowang@zjnu.edu.cn (B. Wang).

https://doi.org/10.1016/j.envpol.2019.06.023
0269-7491/

measurements of saturation isothermal remanent magnetization (SIRM) is an unambiguous indicator of the magnetic mineral concentration and amount of PM deposited on leaves (Hofman et al., 2014a). However, roadside trees play different roles in the retention of airborne PM and have different environmental effects in street canyons and the open road environment, due to differences in ventilation caused by variations in the characteristics of roadside trees (e.g. the thickness and density of the green belt), meteorological and climatic conditions, and the presence of roadside buildings (Gao et al., 2008; Jin et al., 2016). In addition, plant height is an important influencing factor on pollutant reductions in open environments without tall buildings (Abhijith et al., 2017). Therefore, research on the influence of roadside trees on the diffusion of traffic pollutants has especial significance in an open road environment, in the context of refining urban greening strategies.

Previous studies have indicated that the capacity of the leaves of coniferous plants to retain PM was higher than that of deciduous broadleaved species, as a result of their needle morphology (Liang et al., 2016) and the length of exposure. Thus, it has been proposed that coniferous species should be considered in urban greening initiatives in light of their effectiveness in trapping PM (Beckett (Beckett et al., 1998; Beckett et al., 2000a, b). However, the relationship between magnetic characteristics and the weight of PM deposited on conifer needles is poorly understood and no such studies have, to our knowledge, been undertaken in Northwest China. Thus, the aims of the present study are: (1) to explore the spatial distribution characteristics of pollutants on needle surfaces of the roadside tree *Juniperus formosana* in an urban area in semi-arid Northwest China, in order to clarify the variation of the concentration of road pollutants on the horizontal and vertical scales; (2) to establish the nature of the possible relationships between the weight of PM deposited on needles, SIRM and elemental composition; and (3) to evaluate differences in particle retention capacity with differences in tree height and arrangement (i.e. single trees versus rows of trees).

2. Material and methods

2.1. Study area

Lanzhou city is located in Northwest China (Fig. 1a), at the convergence zone between the Tibetan Plateau, Inner Mongolia Plateau and the Chinese Loess Plateau. Lanzhou is situated in a basin surrounded by mountains, at an average elevation of 1500 masl. The most frequent wind directions near the ground surface in Lanzhou are NE, ENE and NNE (Fig. 2a, b) and the annual average wind speed is ~1.24 m s^{-1}, the wind speed during the experimental campaign was ~1.41 m s^{-1} (Lanzhou Meteorological Administration). The city covers an area of ~1088 km^2 and is densely populated (>3 millions persons). In 2017, there were ~1.01 million road vehicles in the Lanzhou area. These vehicles generate large amounts of PM, as a result of fuel combustion, and the wearing of tires, brake pads and other motor vehicle parts. This material contains heavy metals and results in a substantial air pollution problem.

Sampling sites T1 and T2 were located on Beibinhe Road (36°05′25.39″ N, 103°43′58.79″ E) in the Anning district of Lanzhou (Fig. 1b). There were no tall buildings within at least 30 m from the sampling locations and the average traffic volume was typically >60 vehicles per minute, as determined by counting during the sampling period (Fig. 2, c). Sites T1 and T2 were both ~6 m from the road, but they differed in that site T1 included a row of trees, while a solitary tree was sampled at site T2.

2.2. Sampling and analytical methods

2.2.1. Sampling

Samples of the needles of *Juniperus formosana* were collected from two sites in April 2017, before bud-breaking (Fig. 1b). All samples were collected in four directions with respect to the tree trunk: (i) the side facing the road (NE); (ii) the opposite side the road (SW); (iii) the side facing oncoming traffic (NW); and (iv) the side parallel to the direction of traffic flow (SE). In order to ensure uniform sampling height, all samples were collected at heights ranging from 100 to 540 cm, at ~20 cm intervals. 184 needle samples were collected in total.

The needles were not affected by rainfall during the sampling campaign. To avoid possible magnetic differences caused by the maturity of the needles (Hofman et al., 2014b), only mature leaves were collected from the outer canopy. Disposable plastic gloves were used and they were changed after each sample was taken to avoid sample cross-contamination. Needles were tightly packed together using cling film, to prevent movement, and were then

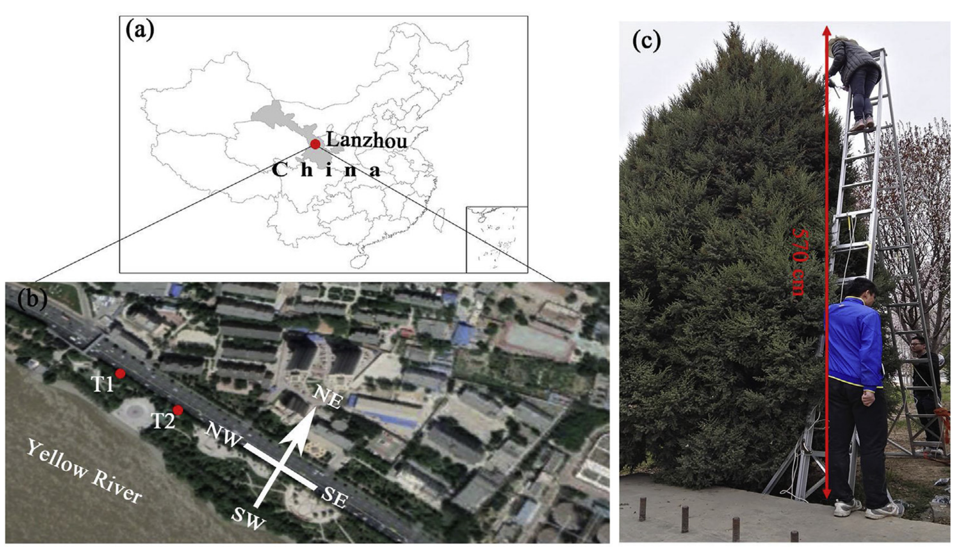

Fig. 1. Location of Lanzhou in China (a). Google Earth image of the sampling locations in Lanzhou (b). Example of an individual of *Juniperus formosana* used for sampling (c). Site T1 included a row of trees, while T2 was a solitary tree. Conifer needles were collected from four directions: NE, the side facing the road; SW, the side opposite the road; NW, the side facing oncoming traffic; and SE, the side parallel to the direction of traffic flow.

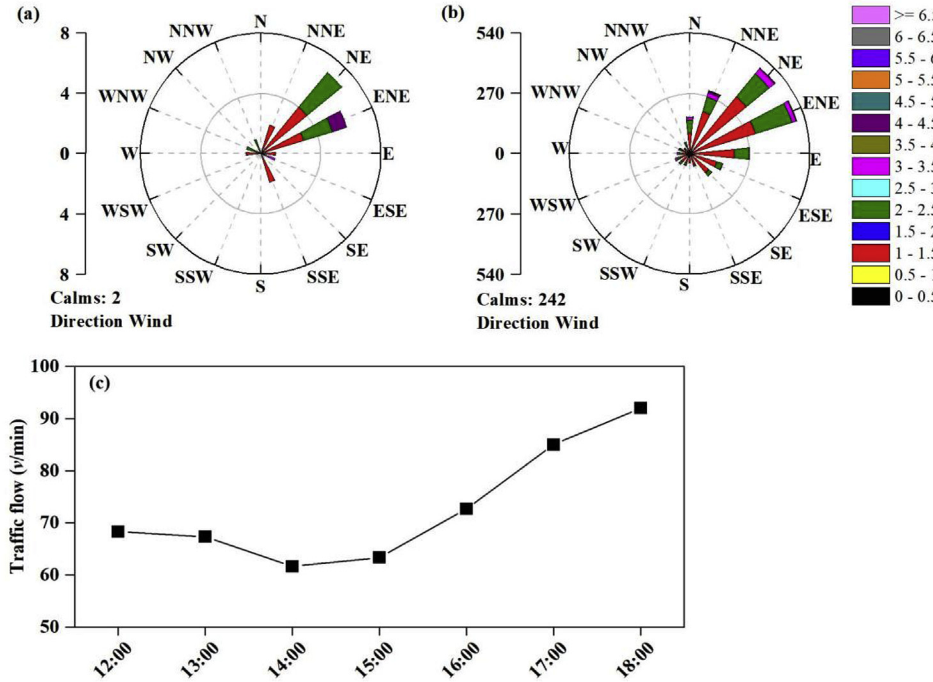

Fig. 2. Wind roses of three-hourly data during the experimental campaigns (a) and during 2016 (b) (data source: Lanzhou Meteorological Administration) and statistics of traffic flow at the studied sites (c).

placed in a plastic container of 8 cm^3 volume. All needle samples were refrigerated at 5 °C prior to transport to the laboratory.

2.2.2. Analytical methods

2.2.2.1. Weight of PM deposited on conifer needles. The weight of PM deposited on needles was detected and analyzed following the elution-filtration method. Needles were washed with distilled water, brushed carefully and then placed in an ultrasonicator (KQ-500DE) for 20 min to ensure the PM was completely removed from the surface. The washings were passed through a nylon sieve (mesh diameter 100 μm) to remove impurities, and then filtered using quartz filters (Whatman, 1851–047). Filter samples were heated to 450 °C in a muffle furnace and weighed before and after dust collection using an electronic balance (accurate to 0.0001 g). The mass of wet *Juniperus formosana* needles was also determined.

2.2.2.2. Magnetic measurements. Unwashed and washed needle samples were magnetized in a direct current (DC) field of 1 T with an MMPM10 pulse magnetizer. The Saturation Isothermal Remanent Magnetization (SIRM) was measured with an AGICO JR6 magnetometer and the resulting values normalized according to wet needle weight ($A \cdot m^2 \cdot kg^{-1}$). The magnetism of the needles was negligible, but its contribution was subtracted from the magnetism of the PM for the unwashed needles to ensure that the SIRM exclusively represented the magnetic signal of PM. SIRM was measured in the Key Laboratory of Western China's Environmental Systems (Ministry of Education), Lanzhou University, China. Representative samples were selected for the measurement of hysteresis loops (in a maximum magnetic field of 1 T) and First order reversal curves (FORC) using a VFTB. The measurements were conducted in the Shanxi Key Laboratory of Disasters Monitoring & Mechanism Simulation, Baoji University of Arts and Sciences.

2.2.2.3. Elemental analysis. Two pieces of quartz filter bearing the PM samples were cut off using a cutting ring with a diameter of 1.5 cm and placed in a PTFE vessel. Samples were then subjected to the following sequential chemical treatments: (i) 6 mL of 65% HNO_3, (ii) 2 mL of concentrated H_2O_2, and (iii) 0.2 mL of 48% HF. The vessel was closed and placed on the rotating turntable of a microwave oven in order to initiate the digestion procedure. The digestion solution was then evaporated using an electric hot plate (BHW–O9A, Shanghai) at 150 °C. Subsequently, 3 mL of 65% HNO_3 was poured into the vessel to perform a further 5 min digestion. The solution was then transferred to a volumetric flask and diluted with 50 mL of deionized water. A standard solution (2 ppm) of rhodium was used as an internal calibration standard for correction of the drift for external calibration curves. A black test was carried out in the same way. The concentrations of Ca, Fe, Al, Mn, Zn, Pb, Cu and Cd were measured using Inductively Coupled Plasma Mass Spectrometry (ICP-MS) in the Lanzhou Center for Oil and Gas Resources, Institute of Geology and Geophysics, CAS.

2.3. Source apportionment method

In order to evaluate the degree of element enrichment in the PM deposited on the needles and to differentiate its sources, the Enrichment factor (*EF*) (Duce et al., 1976) of elements was calculated following equation (1):

$$EF = \frac{(C_i/C_r)particles}{(C_i^{'}\Big/C_r^{'})background} \qquad (1)$$

Here, C_i and C_r are the concentrations of the *i*th element and reference element *r* in the particles, respectively; and $C_i^{'}$ and $C_r^{'}$ are the concentrations of the *i*th element and reference element *r* in the crust, respectively. $EF > 10$ indicates that a given element had been enriched in anthropogenic PM compared to the average concentration present in geological sources. Conversely, where $10 \geq EF > 1$, the elemental composition of the PM indicates a mixture of anthropogenic pollution and natural soil; and where $EF < 1$, the elemental composition mainly reflects dust originating from soil or rock weathering.

2.4. Statistical analysis

Data analysis was performed using SPSS 22.0 (IBM, Solutions Statistical Package for the Social Sciences) and Origin 9.1 (OriginLab). Significant differences in particle retention, SIRM and elemental concentrations between different sampling directions and height ranges were tested using One-way ANOVA. The normality of the data was evaluated statistically using the Kolmogorov-Smirnov Test for Normality, and the results were then transformed using Tukey's Formula in order to meet normality assumptions.

3. Results

3.1. Magnetic characteristics of particles deposited on conifer needles

Hysteresis loop properties reflect the magnetic mineral composition of sample, and the magnetic field strength at which the hysteresis loop is closed indicates the dominant magnetic mineral. The hysteresis loops of the measured samples are tall and thin, and the magnetization increased rapidly with an applied magnetic field between 0 and 250 mT (Fig. 3 a). Hysteresis loops which are closed when the magnetic field is ~250 mT indicate the presence of low coercivity ferromagnetic minerals (Liu et al., 2012). Hysteresis loops which are closed and linear at magnetic fields >250 mT are indicative of contributions from paramagnetic minerals. The respective coercivity (B_c) values of single domain magnetite, multidomain magnetite and hematite are 10 mT, 2 mT and 400 mT, respectively (Thompson and Oldfield, 1986); hence the B_c values of the five representative samples (11.2, 11.0, 11.0, 11.0 and 10.6 mT) are indicative of the presence of canted antiferromagnetic minerals like hematite.

A Day plot shows that all points fall within the pseudo-single-domain (PSD) region (Fig. 3 b). However, the samples may in fact comprise mixtures of grains in different domain states (e.g. single-domain + multidomain (SD + MD) or single-domain + superparamagnetic (SD + SP)) (Roberts et al., 1995), and therefore FORC diagrams were used to check the reliability of the 'Day' plot. The sample contours on the FORC diagram (Fig. 3c, d, e, f, g) show clear evidence of MD + SD particles with characteristic contours that diverge away from the origin (Roberts et al., 2000). Similar FORC diagrams were obtained from PM deposited on roadside plants in Shanghai (Long et al., 2012), in which the central coercivity peak ranged from 20 to 40 mT.

3.2. Relationship between the weight of PM on needles and SIRM

The weight of needles and the SIRM values at different sampling heights in four directions along T1 and T2 are shown in Table 1. The weight of PM deposited on needles ranged from 4.04 $g\,kg^{-1}$ to 49.25 $g\,kg^{-1}$; and the SIRM ranged from $27.61 \times 10^{-5} Am^2 \cdot kg^{-1}$ to $314.46 \times 10^{-5} Am^2 \cdot kg^{-1}$. The weight of PM and the SIRM in the NE direction were always higher than in the SW direction, whilst those in the NW direction were also higher than those in the SE direction. The weight of PM and SIRM in the NE and NW directions, for both T1 and T2, were higher than the average values, apart from those recorded in the NW direction of T1.

One-way ANOVA (Analysis of Variance) was performed on the results from sites T1 and T2 to test whether there were statistically significant variations in the weight of PM and the SIRM on the basis of direction. The results reveal significant differences ($p < 0.0001$) between the four sampling directions, except for SE at site T2 (Table 2).

The correlation results for the weight of PM deposited on needles and SIRM within each direction at sites T1 and T2 are shown in Table 1. In general, the weight of PM is strongly correlated with SIRM ($r = 0.93$, $n = 184$). Statistically significant correlations in individual directions ($p < 0.0001$), apart from in the SE direction at site T2 ($p = 0.0017$), are evident. The correlation in the NE direction is always higher than in the SW direction, and similarly the correlation in the NW direction is higher than in the SE direction. The results therefore show that sampling direction has a significant impact on SIRM (T1, T2: $p < 0.0001$) (Table 2), which in turn reflects the amount of PM deposited on the needles, and hence to the amount of local road traffic emissions and the diffusion of pollutants in an open environment. The results confirm the potential of biomagnetic monitoring as a proxy for the quantity of PM deposited on the surface of needles, as was also shown by the significant correlation between SIRM and the weight of PM deposited on the leaves of London plane (*Platanus* × *acerifolia* Wild) in Antwerp, Belgium (Hofman et al., 2014a).

3.3. Elemental results

The average concentrations of Ca, Fe, Al, Mn, Zn, Pb, Cu and Cd are 616.78 $\mu g\,g^{-1}$, 551.97 $\mu g\,g^{-1}$, 594.42 $\mu g\,g^{-1}$, 10.45 $\mu g\,g^{-1}$, 6.28 $\mu g\,g^{-1}$, 1.83 $\mu g\,g^{-1}$, 1.18 $\mu g\,g^{-1}$ and 0.04 $\mu g\,g^{-1}$, respectively. The concentrations of elements in each direction are shown in Fig. 4. More significant differences between elements measured at site T1 in the four sampling directions are evident compared to site T2 (Table 2). Furthermore, the concentrations of the eight elements are always higher in the NE and NW directions compared to those measured in the SW and SE directions, apart from Mn, Pb, Cu, Cd in the NW direction at site T1.

3.4. Correlation of SIRM and elemental concentrations

The correlations between SIRM and measured elemental concentrations at sites T1 and T2 are shown in Table 3. The correlations are statistically significant ($r = 0.57–0.79$, $p < 0.01$) and they indicate that SIRM is closely related to the elemental concentrations. However, the correlations observed for site T2 ($r = 0.29–0.63$, $p < 0.01$) are lower than for site T1, for all elements. This can be explained by differences in the retention capacities of rows of trees (site T1), as opposed to a single tree (site T2).

4. Discussion

4.1. Distribution of PM deposited on needles and elements

In an open road environment, roadside greening has a significant effect on the diffusion of roadside pollutants by filtering/diluting road pollutants (dust resuspension and traffic exhaust emissions) (Bertolotti and Gialanella, 2014; Chen et al., 2017; Weerakkody et al., 2017; Weerakkody et al., 2018), or by influencing air flow. It was reported that pollutant concentration decreased with increasing distance from the road (Moreno et al., 2003; Prusty et al., 2005). In the study of Hofman et al. (2013) this was also accompanied by a significant reduction in the average SIRM with sampling height (5 m: 29.3×10^{-6} A, 12 m: 10.1×10^{-6} A). However, this study lacked a systematic appraisal of how variations in tree height could affect the retention of PM. In order to test the impact of tree height on the diffusion of PM, the measured changes in SIRM in the NE direction at sites T1 and T2 were clustered using the hierarchical clustering method. The results in the NE direction for site T1 are clustered into three groups, ordered consecutively according

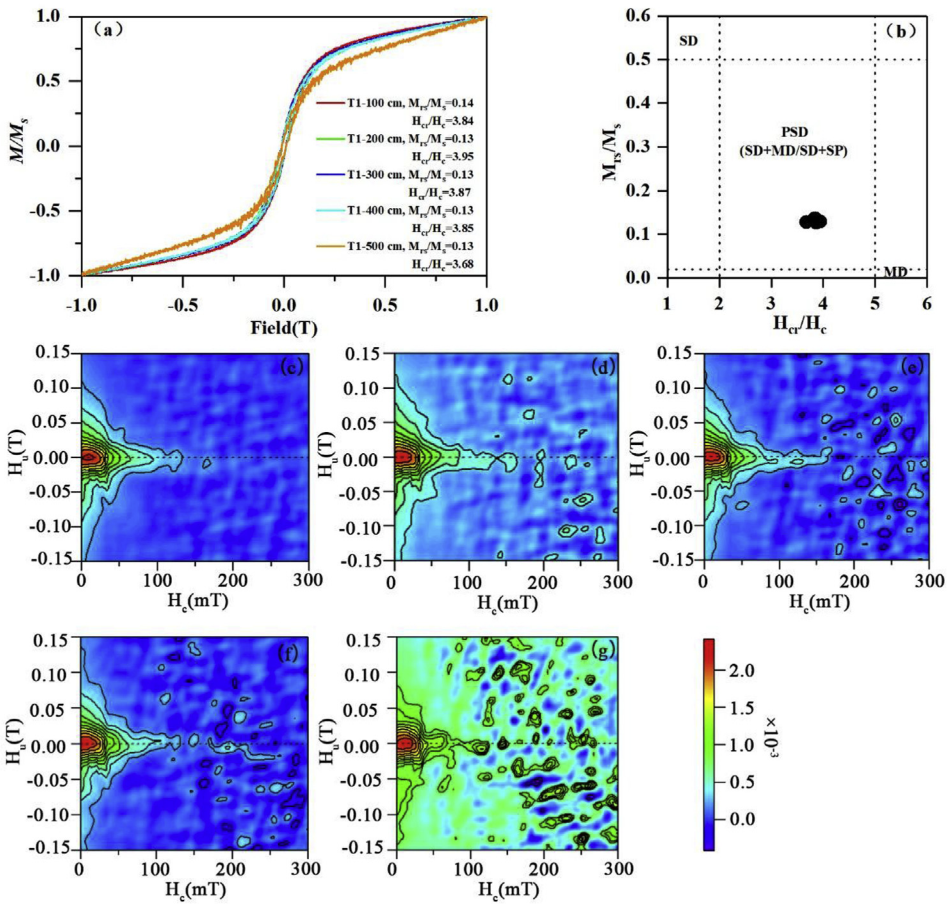

Fig. 3. (a) Hysteresis loops for representative PM samples; (b) corresponding Day plot (modified after Dunlop, 2002); (c–g) FORC diagram for samples at the heights of 100 cm, 200 cm, 300 cm, 400 cm and 500 cm, in the NE direction of T1, respectively. Smoothing factors were set to 10 for all FORC diagrams.

Table 1
Statistics for the weights of PM (W) deposited on needles and corresponding SIRM values, and their statistical relationship, in four directions ($n = 184$). Statistically significant differences are highlighted in bold.

		W ($g \cdot kg^{-1}$)				SIRM ($\times 10^{-5} Am^2 \cdot kg^{-1}$)				Relationship		
		Mean	SD	Min	Max	Mean	SD	Min	Max	r	p-value	Regression equation
	All	15.32	7.25	4.04	49.25	88.77	43.38	27.61	314.46	0.93	< **0.0001**	$F_{(SIRM)} = 5.54 \times W + 3.89$
T1	NE	22.15	12.10	4.78	49.25	141.67	75.88	37.89	314.46	0.96	< **0.0001**	$F_{(SIRM)} = 6.02 \times W + 8.23$
	SW	11.19	4.19	4.49	19.67	61.20	19.83	33.08	104.31	0.83	< **0.0001**	$F_{(SIRM)} = 3.93 \times W + 17.12$
	NW	14.71	6.29	7.00	32.40	95.70	35.13	45.71	170.49	0.96	< **0.0001**	$F_{(SIRM)} = 5.37 \times W + 16.77$
	SE	11.08	4.89	4.04	26.68	68.95	24.36	27.61	122.53	0.95	< **0.0001**	$F_{(SIRM)} = 4.71 \times W + 16.74$
T2	NE	17.74	6.50	9.35	37.77	101.45	27.42	58.88	183.77	0.97	< **0.0001**	$F_{(SIRM)} = 4.10 \times W + 28.67$
	SW	13.17	3.96	7.09	19.19	69.43	19.63	29.12	98.83	0.90	< **0.0001**	$F_{(SIRM)} = 4.45 \times W + 10.76$
	NW	18.08	5.62	7.80	27.33	98.26	27.60	53.59	152.41	0.93	< **0.0001**	$F_{(SIRM)} = 4.57 \times W + 15.61$
	SE	14.43	3.87	7.97	22.85	73.49	26.45	42.04	149.47	0.62	0.0017	$F_{(SIRM)} = 4.21 \times W + 12.72$

to sampling height (Fig. 5). The final cluster members were divided into three height ranges (low (L), medium (M) and high (H); the heights are defined in Fig. 5). We hypothesize that tree height and arrangement are factors leading to different patterns of diffusion and accumulation of road pollutants. To further test this hypothesis, One-way ANOVA was performed between SIRM and element concentrations divided on the basis of height ranges in the NE direction of sites T1 and T2 (Table 4). Significant differences ($p < 0.05$) between particle retention, SIRM and traffic-related element concentrations are evident for site T1, but not for site T2. This indicates that plant configuration may be an important factor affecting the diffusion of pollutants.

In the case of site T1, significantly higher elemental concentrations are observed for PM sampled in the L height range compared with that sampled in the M and H height ranges. In addition, significant differences are observed in different sampling directions along both transects. In particular, the elemental concentrations of PM in the NE direction are higher by factors of 1.41–2.47 and 1.14–1.50 than that in the SW direction for sites T1 and T2, respectively; whereas the elemental concentrations of PM deposited in the NW direction are higher by factors of 1.33–1.54 and 1.28–1.62 than that in the SE direction for sites T1 and T2, respectively.

Significant differences are also evident between sites T1 and T2.

Table 2
Results of One-way ANOVA performed between four sampling directions (NE, SW, NW and SE) at sites T1 and T2. Statistically significant differences ($p < 0.0001$) are highlighted in bold.

	T1		T2	
	F	*p*-valve	F	*p*-valve
W	8.355	**< 0.0001**	5.290	0.002
SIRM	14.461	**< 0.0001**	11.491	**< 0.0001**
Ca	6.412	0.01	4.918	0.003
Fe	9.403	**< 0.0001**	4.334	0.007
Al	11.062	**< 0.0001**	2.539	0.062
Mn	9.337	**< 0.0001**	4.630	0.005
Zn	11.293	**< 0.0001**	3.867	0.012
Pb	7.397	**< 0.0001**	5.199	0.002
Cu	5.895	0.001	6.283	0.001
Cd	5.438	0.002	2.295	0.083

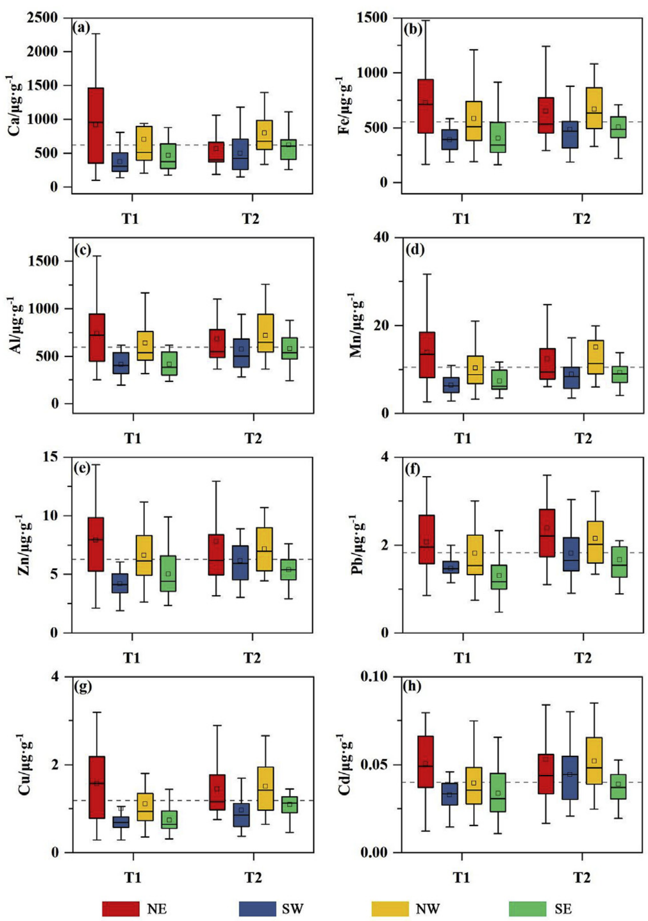

Fig. 4. Box and whisker plots showing the concentrations of elements in PM deposited on needles collected from four directions at sites T1 and T2. The dashed lines are mean values. (a–h: Ca, Fe, Al, Mn, Zn, Pb, Cu and Cd, respectively).

The elemental concentrations of PM deposited at site T1 are higher than at site T2, at heights L and M, in the NE direction; however, by contrast, the elemental concentrations at site T1 are lower than at site T2 at height H. In the other three directions, at heights M and H, the elemental concentrations of PM along site T1 are lower than at site T2.

It is well documented that PM in air is often contaminated by a range of elements which are hazardous to human health. Measurements of the magnetic and elemental composition of PM deposited on needles has been considered to be an effective alternative to active monitoring with improved spatial resolution (Ram et al., 2015). Atmospheric particles usually contain trace elements which originate from both natural and anthropogenic sources. The results of previous magnetic studies have demonstrated that the magnetic properties of PM deposited on needles was dominated by coarse-grained ferromagnetic minerals derived from both traffic exhaust emissions and non-combustion sources (Baldacchini et al., 2017; Jordanova et al., 2014; Wang et al., 2012). In addition, *EF* was used to identify and evaluate the relative contributions of natural and anthropogenic sources to the PM, on the basis of Ca, Fe, Mn, Zn, Pb, and Cu concentrations. In the present study, Al was selected as a reference element on the basis of its abundance in geological sources and in topsoil close to Lanzhou (Fig. 6). The results of *EF* analysis are essentially consistent irrespective of direction at sites T1 and T2. The mean values of *EF* for Ca, Fe, Mn, Cu and Cd are 1.40, 1.88, 1.66, 5.19 and 4.02, respectively. These results indicate that the concentrations of Ca, Fe and Mn reflect mixtures of anthropogenic pollutants and soils, whereas Cu and Cd are dominated by anthropogenic sources. The mean *EF* of elements Pb and Zn are 10.45, 10.72, respectively, which indicates the substantial enrichment of PM by anthropogenic pollutants. In general, the concentrations of Mn, Zn, Pb, Cu, Cd are mainly controlled by road traffic. The largest sources of Cd, Zn and Cu were determined to be vehicle brakes and lubricants (Duan and Tan, 2013; Vallius et al., 2003), whereas the main sources of Mn, Pb and Zn were traffic exhaust emissions. These data show that PM composition mainly reflects the continuous accumulation of resuspended dust and particles from traffic exhaust emissions. However, moving vehicles and roadside trees disturb the ambient air flow, which has also been shown to affect the diffusion of pollutants.

The results of *EF* vary significantly with tree height, but variations in crustal elements are still clearly distinguished from anthropogenic elements. As shown in Fig. 6, the *EF* value of Ca at height range L is higher than in height ranges M and H. Furthermore, a decrease in the *EF* of Ca is observed with increasing height along the NE, SW and NW directions at site T1. There are no significant differences in the *EF* of Fe and Mn between the three height ranges. However, the highest *EF* values of Pb, Zn, Cu and Cd occur at height ranges M or H, apart from Pb and Zn in the SW direction. In particular, the *EF* values of Cu and Cd in the NW direction at site T2 indicate that the PM close to the ground was strongly impacted by dust re-suspension. Elements indicative of geological sources are found to have diluted the traffic-related elements, resulting in lower values of *EF* for Pb, Zn, Cu and Cd at lower heights (range L).

Unlike the *EF* results, the concentration of remanence-bearing ferrimagnets (SIRM) decreases with height (Fig. 7). Although SIRM is overall significantly correlated with the measured element concentrations, it may not respond sensitively to the enrichment of specific elements.

4.2. Tree configuration and road pollutant diffusion

Compositional analyses of particles deposited on the surfaces of leaves have been widely used for monitoring ambient atmospheric pollution levels (Baldacchini et al., 2017; Beckett et al., 1998; Blanusa et al., 2015; Burkhardt and Grantz, 2016; Chen et al., 2017; Ram et al., 2012; Sgrigna et al., 2015; Simon et al., 2014), and have been incorporated into pollutant dispersion models (Hofman et al., 2013; Jeanjean et al., 2016; Selmi et al., 2016). In addition, the capacity for PM retention and distribution of trace elements is significantly affected by leaf morphology (Liu et al., 2018; Ram et al., 2012; Simon et al., 2014). Previous studies have shown that the PM retention capacity of coniferous species was higher than that of broadleaved species, as a result of their more complex foliage

Table 3
Correlation between SIRM and elemental concentrations of PM deposited on needles in four directions at sites T1 and T2.

	T1									T2								
	SIRM	Ca	Fe	Al	Mn	Zn	Pb	Cu	Cd	SIRM	Ca	Fe	Al	Mn	Zn	Pb	Cu	Cd
SIRM	1									1								
Ca	0.79**	1								0.60**	1							
Fe	0.75**	0.96**	1							0.63**	0.85**	1						
Al	0.73**	0.95**	0.99**	1						0.61**	0.87**	0.95**	1					
Mn	0.76**	0.97**	0.99**	0.98**	1					0.29**	0.47**	0.66**	0.51**	1				
Zn	0.73**	0.92**	0.96**	0.95**	0.95**	1				0.55**	0.61**	0.77**	0.75**	0.43**	1			
Pb	0.67**	0.83**	0.91**	0.89**	0.88**	0.88**	1			0.63**	0.71**	0.89**	0.87**	0.47**	0.80**	1		
Cu	0.57**	0.71**	0.72**	0.71**	0.72**	0.68**	0.66**	1		0.52**	0.70**	0.91**	0.82**	0.82**	0.69**	0.75**	1	
Cd	0.72**	0.88**	0.93**	0.91**	0.91**	0.93**	0.90**	0.68**	1	0.60**	0.76**	0.89**	0.88**	0.48**	0.75**	0.93**	0.73**	1

**: correlation is significant at the 0.01 level (two-tailed).
*: correlation is significant at the 0.05 level (two-tailed).

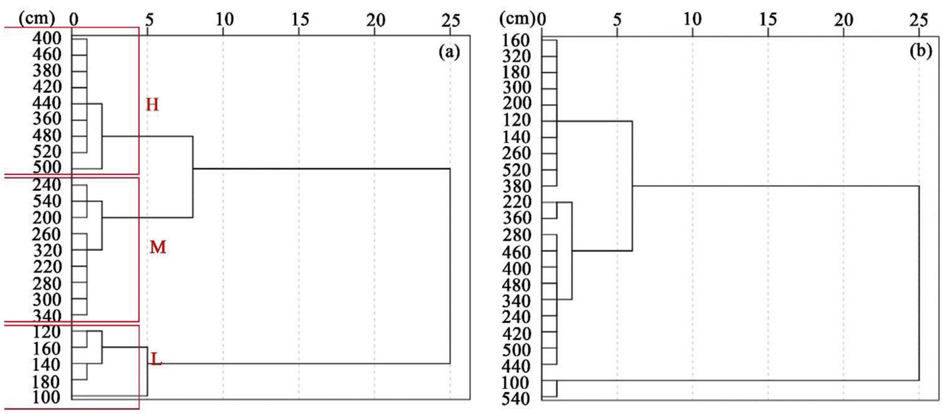

Fig. 5. Hierarchical cluster plot of SIRM in the NE direction of site T1 (a) and site T2 (b) for different sampling heights. (Hclust*, "ward. 'D', L: 100–180 cm; M: 200–340 cm; H: 360–540 cm. The sample at 540cm height was included within range H for continuity in height..)

Table 4
Results of One-way ANOVA of particle retention (*W*), SIRM and element concentrations at different height ranges, L ($n = 5$), M ($n = 8$) and H ($n = 10$). Significant differences ($p < 0.0001$) are shown in bold.

Parameter	T1-NE		T2-NE	
	F-value	p-value	F-value	p-value
W	88.728	< **0.0001**	3.952	0.036
SIRM	63.416	< **0.0001**	4.451	0.025
Ca	18.367	< **0.0001**	0.304	0.741
Fe	6.432	0.007	0.514	0.606
Al	5.424	0.012	0.748	0.486
Mn	6.005	0.009	0.659	0.528
Zn	6.382	0.007	0.991	0.389
Pb	4.793	0.02	2.428	0.114
Cu	8.839	0.002	1.052	0.368
Cd	5.78	0.01	3.476	0.051

structure which facilitates the interception of PM (Bertolotti and Gialanella, 2014; Song et al., 2015; Xie et al., 2018). It has been widely observed that the particles on leaf surfaces in an urban roadside canyon were significantly affected by the distance from the traffic source, as well as by tree crown characteristics (Hofman et al., 2016; Hofman et al., 2013; Hofman et al., 2014a; Simon et al., 2014). In addition, roadside trees can reduce the pollutants derived from traffic via pollutant retention on leaves within the tree canopy. Previous research has indicated that height and canopy characteristics were key factors affecting the capacity of leaves to accumulate PMs (Simon et al., 2014), and thus that changes in PM concentration on the same tree could reflect different dynamic processes under different wind speed conditions (Xie et al., 2018).

In this study, tree configuration could also be a key factor leading to differential particle retention capacity by different needles. As shown in Fig. 6, the decreasing weight of PM deposited on needles and decreasing SIRM at Site T1 can be observed with increasing height (L > M > H), with values higher by factors of 1.46–3.31 and 1.98–3.58 higher at height L than at height H, respectively. Furthermore, the weight of PM and the SIRM values at both sites T1 and T2 are higher in the NE and NW directions compared to the SW and SE directions.

It is also evident that there are differences in the weight of PM and SIRM in four directions and at the three heights between sites T1 and T2 (Fig. 7): (i) At height L, the SIRM and PM are higher at site T1 than at site T2, especially in the NE and NW directions; (ii) at height M, the values for site T1 are higher than those for site T2 in the NE direction only; and (iii) the values at site T1 are lower than at site T2, irrespective of direction at height H. In addition, the observed statistically significant variations in SIRM with height in the NE direction at site T1 indicate that the amount of pollutants gradually decreased with increasing height. In particular, SIRM at height H in the NE direction decreased by 69.31% for site T1 while the SIRM at height H only decreased by 21.44% at site T2; this indicates that more pollutants reached higher elevations at site T2 than at site T1 (at heights M and H). The results indicate large differences in the quantity of PM retained by trees of different configuration, which has impacted the dispersion and filtration of pollutants. Evidently, rows of trees act as a better filter, trapping more road traffic pollutants below height M (~340 cm) (especially at heights less than 200 cm) than the case for a solitary tree, where the PM diffuses to higher elevations. Therefore, tree configuration is

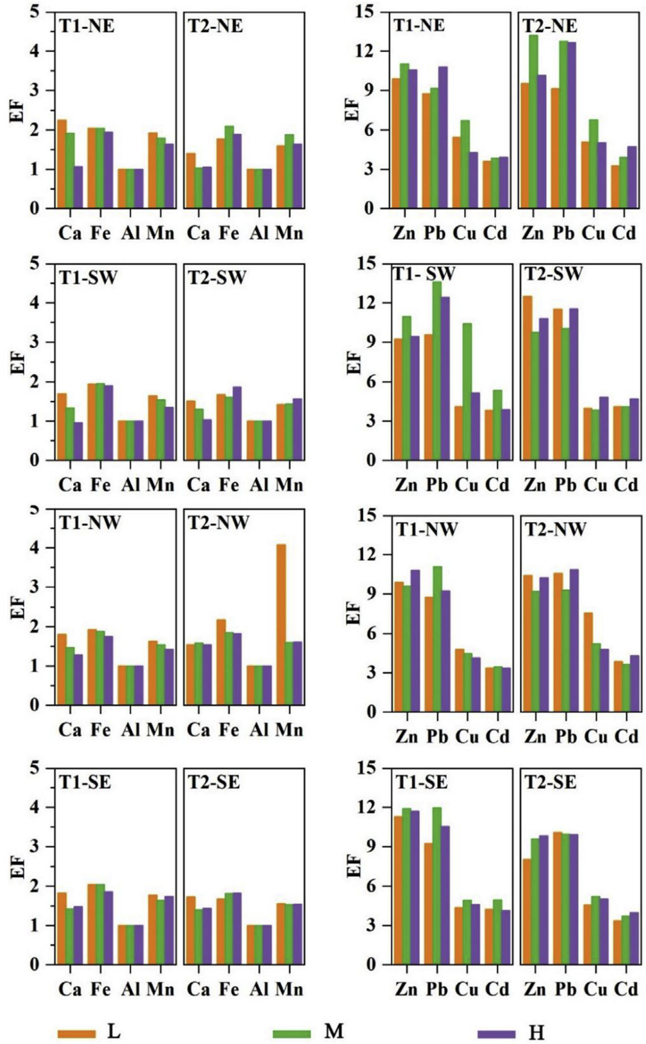

Fig. 6. EF of eight elements and SIRM values at three sampling heights (L, M, H) in four directions at sites T1 and T2.

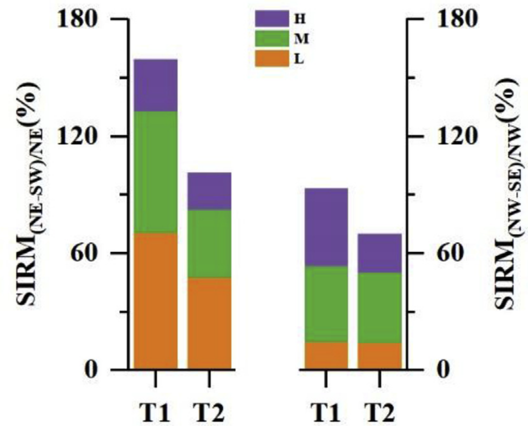

Fig. 8. SIRM differences for NE *vs* SW and NW *vs* SE directions at three heights for sites T1 and T2.

a key factor influencing the distribution and concentration of pollutants.

To further evaluate the effect of roadside trees on the diffusion of traffic pollutants, the ratio of the SIRM of PM in two opposite directions was calculated. The values of $SIRM_{(NE-SW)/NE}$ at site T1 are 70.51%, 62.42% and 26.42% at heights L, M and H, respectively (Fig. 8); and the equivalent values of $SIRM_{(NE-SW)/NE}$ for site T2 are 47.70%, 34.63% and 18.88%. SIRM is higher in the NE direction than in the SW direction at both sites, but $SIRM_{(NE-SW)/NE}$ at site T1 is always higher than at site T2. This may be because roadside vegetation acts as an effective biological barrier (Al-Dabbous and Kumar, 2014; Baldauf, 2017): previous results have shown that denser vegetation reduces atmospheric pollution levels (Al-Dabbous and Kumar, 2014), and that traffic pollutants are trapped by vegetation barriers that are dense with full coverage from the ground to the top of the *Juniperus formosana* canopy. Consequently, rows of bushy closely-spaced trees are more effective at trapping pollutants than a solitary tree. And in the process of road pollutant diffusion, wind direction and speed are additional important factors that should be considered (Al-Dabbous and Kumar, 2014; Uni and Katra,

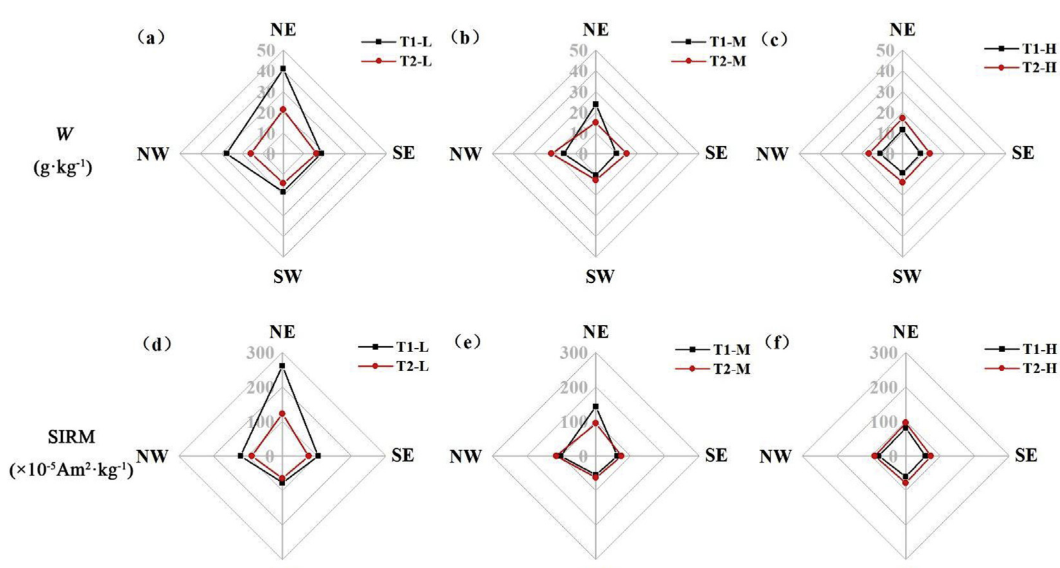

Fig. 7. wt of PM deposited on needles and SIRM values, in four directions and at three height ranges at sites T1 and T2.

2017; Xie et al., 2018), as shown in Fig. 2, one of the most frequent wind directions near the ground surface is NE, which results in the accumulation of larger quantities on the tree leaves in the windward (NE) than that in the leeside (SW), even if low wind speeds occurred in this study.

The results indicate that the processes of PM accumulation on the surfaces of tree needles are complex, mainly controlled by tree configuration that influences the process of road pollutant diffusion in an open road environment. However, as shown in Fig. 8, SIRM in the NW direction was higher than in the SE direction, and the largest value of $SIRM_{(NW-SE)/NW}$ is observed at height M for both sites T1 and T2, indicating that higher SIRM occurs in the NW direction (the side facing oncoming traffic) than in the SE direction (the side parallel to the direction of traffic flow) at both sites. Due to one of the predominant wind directions is NNE, then the transport of pollutant in this direction could induce higher deposition on tree leaves in the NW direction than in the SE direction. Additionally, for very low wind speed scenarios, the movement of vehicle could influence on the direction of pollutant transportation and dispersion.

5. Conclusions

(1) Strong correlations ($r = 0.62–0.97$, $p < 0.05$) were observed between the weight of PM deposited on conifer needles of roadside trees and SIRM within various directions at two sites in a typical semi-arid urban area of Lanzhou, Northwest China. This result confirms the potential of biomagnetic monitoring as a proxy for the quantity of particles deposited on the surface of needles.

(2) High *EF* values of Pb, Zn, Cd and Cu indicate the clear enrichment of PM by anthropogenic pollutants. It is likely that PM composition mainly reflects the continuous accumulation of resuspended dust and particles from road vehicle exhaust emissions. However, elements indicative of geological sources preserved in the PM were enriched on leaves at lower elevations, thus diluting the concentrations of trace elements indicative of anthropogenic sources.

(3) Significant differences ($p < 0.05$) between PM retention, SIRM and traffic-related elements were found for rows of trees, but not for a solitary tree, at three height ranges in the NE direction (road-facing side) of the two sites, suggesting that tree configuration is an important factor affecting the horizontal and vertical diffusion of pollutants. It is likely that both moving vehicles and roadside trees disturbed the ambient air flow, which has also been shown to affect the diffusion of pollutants. Road pollutants were mainly concentrated on the needles of rows of trees below 340 cm height (especially below 200 cm) on the sides facing the road. In addition, decreasing concentrations of pollutants were observed with increasing elevation above the road surface. In general, tree configuration is shown to be the most important factor affecting the accumulation and diffusion of road pollutants in an open environment.

Acknowledgements

We thank Dr. Jan Bloemendal in University of Liverpool for critical discussions, constructive suggestions and English improvement.

Appendix A. Supplementary data

Supplementary data to this article can be found online at https://doi.org/10.1016/j.envpol.2019.06.023.

Funding

This work was supported by the National Natural Science Foundation of China (grant 41504056 and 41877444), the Science-technology Support Plan Projects of Gansu province (grant 1604FKCA096), and China Postdoctoral Science Foundation (grant 2015M580892, 2017T100785).

Declaration of interests

None.

References

Abhijith, K.V., Kumar, P., Gallagher, J., McNabola, A., Baldauf, R., Pilla, F., Broderick, B., Di Sabatino, S., Pulvirenti, B., 2017. Air pollution abatement performances of green infrastructure in open road and built-up street canyon environments – a review. Atmos. Environ. 162, 71–86.
Al-Dabbous, A.N., Kumar, P., 2014. The influence of roadside vegetation barriers on airborne nanoparticles and pedestrians exposure under varying wind conditions. Atmos. Environ. 90, 113–124.
Baldacchini, C., Castanheiro, A., Maghakyan, N., Sgrigna, G., Verhelst, J., Alonso, R., Amorim, J.H., Bellan, P., Bojovic, D.D., Breuste, J., Buhler, O., Cantar, I.C., Carinanos, P., Carriero, G., Churkina, G., Dinca, L., Esposito, R., Gawronski, S.W., Kern, M., Le Thiec, D., Moretti, M., Ningal, T., Rantzoudi, E.C., Sinjur, I., Stojanova, B., Anicic Urosevic, M., Velikova, V., Zivojinovic, I., Sahakyan, L., Calfapietra, C., Samson, R., 2017. How does the amount and composition of PM deposited on platanus acerifolia leaves change across different cities in europe? Environ. Sci. Technol. 51, 1147–1156.
Baldauf, R., 2017. Roadside vegetation design characteristics that can improve local, near-road air quality. Transport. Res. Transport Environ. 52, 354–361.
Beckett, K.P., Freer-Smith, P.H., Taylor, G., 1998. Urban woodlands: their role in reducing the effects of particulate pollution. Environ. Pollut. 99, 347–360.
Beckett, K.P., Freer-Smith, P.H., Taylor, G., 2000a. Effective tree species for local air quality management. J. Arboric. 26, 12–19.
Beckett, K.P., Freer-Smith, P.H., Taylor, G., 2000b. Particulate pollution capture by urban trees: effect of species and wind speed. Glob. Chang. Biol. 6, 995–1003.
Bertolotti, G., Gialanella, S., 2014. Review: use of conifer needles as passive samplers of inorganic pollutants in air quality monitoring. Analytical Methods 6, 6208–6222.
Blanusa, T., Fantozzi, F., Monaci, F., Bargagli, R., 2015. Leaf trapping and retention of particles by holm oak and other common tree species in Mediterranean urban environments. Urban For. Urban Green. 14, 1095–1101.
Burkhardt, J., 2010. Hygroscopic particles on leaves: nutrients or desiccants? Ecol. Monogr. 80, 369–399.
Burkhardt, J., Grantz, D.A., 2016. Plants and Atmospheric Aerosols 78, 369–406.
Burkhardt, J., Pariyar, S., 2014. Particulate pollutants are capable to 'degrade' epicuticular waxes and to decrease the drought tolerance of Scots pine (Pinus sylvestris L.). Environ. Pollut. 184, 659–667.
Chen, L.X., Liu, C.M., Zhang, L., Zou, R., Zhang, Z.Q., 2017. Variation in tree species ability to capture and retain airborne fine particulate matter (PM2.5). Sci. Rep. 7, 3206, 3210.1038/s41598-41017-03360-41591.
Duan, J.C., Tan, J.H., 2013. Atmospheric heavy metals and Arsenic in China: situation, sources and control policies. Atmos. Environ. 74, 93–101.
Duce, R.A., Hoffman, G.L., Ray, B.J., Fletcher, I.S., Wallace, G.T., Fasching, J.L., Piotrowicz, S.R., Walsh, P.R., Hoffman, E.J., 1976. Trace Metals in the Marine Atmosphere: Sources and Fluxes ([Pollutants]).
Gao, N.P., Niu, J.L., Perino, M., Heiselberg, P., 2008. The airborne transmission of infection between flats in high-rise residential buildings: tracer gas simulation. Build. Environ. 43, 1805–1817.
Gautam, P., Blaha, U., Appel, E., 2005. Magnetic susceptibility of dust-loaded leaves as a proxy of traffic-related heavy metal pollution in Kathmandu city, Nepal. Atmos. Environ. 39, 2201–2211.
Hart, J.E., Rimm, E.B., Rexrode, K.M., Laden, F., 2013. Changes in traffic exposure and the risk of incident myocardial infarction and all-cause mortality. Epidemiology 24, 734–742.
Hofman, J., Bartholomeus, H., Janssen, S., Calders, K., Wuyts, K., Wittenberghe, S.V., Samson, R., 2016. Influence of tree crown characteristics on the local PM 10 distribution inside an urban street canyon in Antwerp (Belgium): a model and experimental approach. Urban For. Urban Green. 20, 265–276.
Hofman, J., Stokkaer, I., Snauwaert, L., Samson, R., 2013. Spatial distribution assessment of particulate matter in an urban street canyon using biomagnetic leaf monitoring of tree crown deposited particles. Environ. Pollut. 183, 123–132.
Hofman, J., Wuyts, K., Van Wittenberghe, S., Brackx, M., Samson, R., 2014a. On the link between biomagnetic monitoring and leaf-deposited dust load of urban trees: relationships and spatial variability of different particle size fractions. Environ. Pollut. 189, 63–72.
Hofman, J., Wuyts, K., Van Wittenberghe, S., Samson, R., 2014b. On the temporal variation of leaf magnetic parameters: seasonal accumulation of leaf-deposited and leaf-encapsulated particles of a roadside tree crown. Sci. Total Environ. 493,

766–772.

Huang, J., Guo, X.B., 2014. Research progress on the health effects of traffic-related air pollution. China Environ. Sci. 34, 1592–1598.

Jeanjean, A.P.R., Monks, P.S., Leigh, R.J., 2016. Modelling the effectiveness of urban trees and grass on PM 2.5 reduction via dispersion and deposition at a city scale. Atmos. Environ. 147, 1–10.

Jin, X., Yang, L., Du, X., Yang, Y., 2016. Transport characteristics of PM2.5 inside urban street canyons: the effects of trees and vehicles. Building Simulation 10, 337–350.

Jones, A.Y., Lam, P.K., Dean, E., 2006. Respiratory health of bus drivers in Hong Kong. Int. Arch. Occup. Environ. Health 79, 414–418.

Jordanova, D., Jordanova, N., Petrov, P., 2014. Magnetic susceptibility of road deposited sediments at a national scale–relation to population size and urban pollution. Environ. Pollut. 189, 239–251.

Karagulian, F., Belis, C.A., Dora, C.F.C., Prüss-Ustün, A.M., Bonjour, S., Adair-Rohani, H., Amann, M., 2015. Contributions to cities' ambient particulate matter (PM): a systematic review of local source contributions at global level. Atmos. Environ. 120, 475–483.

Kardel, F., Wuyts, K., Babanezhad, M., Vitharana, U.W., Wuytack, T., Potters, G., Samson, R., 2010. Assessing urban habitat quality based on specific leaf area and stomatal characteristics of Plantago lanceolata L. Environ. Pollut. 158, 788–794.

Liang, D., Ma, C., Wang, Y.Q., Wang, Y.J., Chen-xi, Z., 2016. Quantifying PM2.5 capture capability of greening trees based on leaf factors analyzing. Environ. Sci. Pollut. Res. Int. 23, 21176–21186.

Litschke, T., Kuttler, W., 2008. On the reduction of urban particle concentration by vegetation a review. Meteorol. Z. 17, 229–240.

Liu, J.Q., Cao, Z.G., Zou, S.Y., Liu, H.H., Hai, X., Wang, S.H., Duan, J., Xi, B.Y., Yan, G.X., Zhang, S.W., Jia, Z.K., 2018. An investigation of the leaf retention capacity, efficiency and mechanism for atmospheric particulate matter of five greening tree species in Beijing, China. Sci. Total Environ. 616–617, 417–426.

Liu, Q.S., Roberts, A.P., Larrasoaña, J.C., Banerjee, S.K., Guyodo, Y., Tauxe, L., Oldfield, F., 2012. Environmental magnetism: principles and applications. Rev. Geophys. 50 (RG4002), 4001–4050.

Long, Q., Zhou, J.Z., Meng, J., Da, L.J., 2012. Magnetic response of street tree leaves to particulate pollution in Shanghai. Environmental science 33, 4188–4193.

Moreno, E., Sagnotti, L., Dinarès-Turell, J., Winkler, A., Cascella, A., 2003. Biomonitoring of traffic air pollution in Rome using magnetic properties of tree leaves. Atmos. Environ. 37, 2967–2977.

Prajapati, S.K., Pandey, S.K., Tripathi, B.D., 2006. Monitoring of vehicles derived particulates using magnetic properties of leaves. Environ. Monit. Assess. 120, 169–175.

Prusty, B.A., Mishra, P.C., Azeez, P.A., 2005. Dust accumulation and leaf pigment content in vegetation near the national highway at Sambalpur, Orissa, India. Ecotoxicol. Environ. Saf. 60, 228–235.

Rai, P.K., 2013. Environmental magnetic studies of particulates with special reference to biomagnetic monitoring using roadside plant leaves. Atmos. Environ. 72, 113–129.

Ram, S.S., Majumder, S., Chaudhuri, P., Chanda, S., Santra, S.C., Chakraborty, A., Sudarshan, M., 2015. A review on air pollution monitoring and management using plants with special reference to foliar dust adsorption and physiological stress responses. Crit. Rev. Environ. Sci. Technol. 45, 2489–2522.

Ram, S.S., Majumder, S., Chaudhuri, P., Chanda, S., Santra, S.C., Maiti, P.K., Sudarshan, M., Chakraborty, A., 2012. Plant canopies: bio-monitor and trap for re-suspended dust particulates contaminated with heavy metals. Mitig. Adapt. Strategies Glob. Change 19, 499–508.

Roberts, A.P., Cui, Y., Verosub, K.L., 1995. Wasp-waisted hysteresis loops: mineral magnetic characteristics and discrimination of components in mixed magnetic systems. J. Geophys. Res.: Solid Earth 100, 17909–17924.

Roberts, A.P., Pike, C.R., Verosub, K.L., 2000. First-order reversal curve diagrams: a new tool for characterizing the magnetic properties of natural samples. J. Geophys. Res.: Solid Earth 105, 28461–28475.

Selmi, W., Weber, C., Rivière, E., Blond, N., Mehdi, L., Nowak, D., 2016. Air pollution removal by trees in public green spaces in Strasbourg city, France. Urban For. Urban Green. 17, 192–201.

Sgrigna, G., Saebo, A., Gawronski, S., Popek, R., Calfapietra, C., 2015. Particulate Matter deposition on Quercus ilex leaves in an industrial city of central Italy. Environ. Pollut. 197, 187–194.

Simon, E., Baranyai, E., Braun, M., Cserhati, C., Fabian, I., Tothmeresz, B., 2014. Elemental concentrations in deposited dust on leaves along an urbanization gradient. Sci. Total Environ. 490, 514–520.

Song, Y., Maher, B.A., Li, F., Wang, X., Sun, X., Zhang, H., 2015. Particulate matter deposited on leaf of five evergreen species in Beijing, China: source identification and size distribution. Atmos. Environ. 105, 53–60.

Szönyi, M., Sagnotti, L., Hirt, A.M., 2007. On leaf magnetic homogeneity in particulate matter biomonitoring studies. Geophys. Res. Lett. 34, L06306, 06310.01029/02006GL029076.

Thompson, R., Oldfield, F., 1986. Environmental Magnetism. Allen& Unwin, London, pp. 1–127.

Uni, D., Katra, I., 2017. Airborne dust absorption by semi-arid forests reduces PM pollution in nearby urban environments. Sci. Total Environ. 598, 984–992.

Urbat, M., Lehndorff, E., Schwark, L., 2004. Biomonitoring of air quality in the Cologne conurbation using pine needles as a passive sampler-Part I: magnetic properties. Atmos. Environ. 38, 3781–3792.

Vallius, M., Lanki, T., Tiittanen, P., Koistinen, K., Ruuskanen, J., Pekkanen, J., 2003. Source apportionment of urban ambient PM 2.5 in two successive measurement campaigns in Helsinki, Finland? Atmos. Environ. 37, 615–623.

Wang, B., Xia, D.S., Yu, Y., Jia, J., Xu, S.J., 2012. Magnetic records of heavy metal pollution in urban topsoil in Lanzhou, China. Chin. Sci. Bull. 58, 384–395.

Weerakkody, U., Dover, J.W., Mitchell, P., Reiling, K., 2017. Particulate matter pollution captured by leaves of seventeen living wall species with special reference to rail-traffic at a metropolitan station. Urban For. Urban Green. 27, 173–186.

Weerakkody, U., Dover, J.W., Mitchell, P., Reiling, K., 2018. Quantification of the traffic-generated particulate matter capture by plant species in a living wall and evaluation of the important leaf characteristics. Sci. Total Environ. 635, 1012–1024.

Wu, S.W., Deng, F.R., Huang, J., Wang, H.Y., Shima, M., Wang, X., Qin, Y., Zheng, C.J., Wei, H.Y., Hao, Y., Lv, H.B., Lu, X.L., Guo, X.B., 2013. Blood pressure changes and chemical constituents of particulate air pollution: results from the healthy volunteer natural relocation (HVNR) study. Environ. Health Perspect. 121, 66–72.

Wu, S.W., Deng, F.R., Wei, H.Y., Huang, J., Wang, H.Y., Shima, M., Wang, X., Qin, Y., Zheng, C.J., Hao, Y., Guo, X.B., 2012. Chemical constituents of ambient particulate air pollution and biomarkers of inflammation, coagulation and homocysteine in healthy adults: a prospective panel study. Part. Fibre Toxicol. 9, 49. http://www.particleandfibretoxicology.com/content/9/1/49.

Xie, C.K., Kan, L.Y., Guo, J.K., Jin, S.J., Li, Z.G., Chen, D., Li, X., Che, S.Q., 2018. A dynamic processes study of PM retention by trees under different wind conditions. Environ. Pollut. 233, 315–322.